Probing Trions at Chemically Tailored Trapping Defects

Hyejin Kwon,[†,#] Mijin Kim,[†,#] Manuel Nutz,[‡] Nicolai F. Hartmann,[§] Vivien Perrin,[‡] Brendan Meany,[†] Matthias S. Hofmann,[‡] Charles W. Clark,[∥] Han Htoon,[§] Stephen K. Doorn,[§] Alexander Högele,[‡] and YuHuang Wang[*,†,⊥]

[†]Department of Chemistry and Biochemistry, University of Maryland, 8051 Regents Drive, College Park, Maryland 20742, United States

[‡]Fakultat für Physik, Center for NanoScience and Munich Quantum Center, Ludwig-Maximilians-Universitat München, Geschwister-Scholl-Platz 1, D-80539 München, Germany

[§]Center for Integrated Nanotechnologies, Materials Physics and Applications Division, Los Alamos National Laboratory, Los Alamos, New Mexico 87545, United States

[∥]Joint Quantum Institute, National Institute of Standards and Technology, Gaithersburg, Maryland 20902, United States

[⊥]Maryland NanoCenter, University of Maryland, College Park, Maryland 20742, United States

S *Supporting Information*

ABSTRACT: Trions, charged excitons that are reminiscent of hydrogen and positronium ions, have been intensively studied for energy harvesting, light-emitting diodes, lasing, and quantum computing applications because of their inherent connection with electron spin and dark excitons. However, these quasi-particles are typically present as a minority species at room temperature making it difficult for quantitative experimental measurements. Here, we show that by chemically engineering the well depth of sp^3 quantum defects through a series of alkyl functional groups covalently attached to semiconducting carbon nanotube hosts, trions can be

efficiently generated and localized at the trapping chemical defects. The exciton-electron binding energy of the trapped trion approaches 119 meV, which more than doubles that of "free" trions in the same host material (54 meV) and other nanoscale systems (2−45 meV). Magnetoluminescence spectroscopy suggests the absence of dark states in the energetic vicinity of trapped trions. Unexpectedly, the trapped trions are approximately 7.3-fold brighter than the brightest previously reported and 16 times as bright as native nanotube excitons, with a photoluminescence lifetime that is more than 100 times larger than that of free trions. These intriguing observations are understood by an efficient conversion of dark excitons to bright trions at the defect sites. This work makes trions synthetically accessible and uncovers the rich photophysics of these tricarrier quasi-particles, which may find broad implications in bioimaging, chemical sensing, energy harvesting, and light emitting in the short-wave infrared.
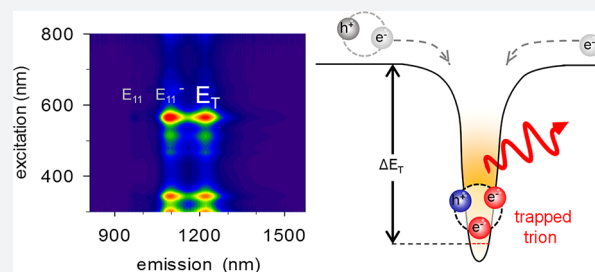
INTRODUCTION

A negative trion is an electron−hole−electron (e−h−e) tricarrier quasi-particle that is reminiscent of hydrogen and positronium ions.[1] In contrast to electron−hole pairs that are known as excitons, a trion features a net charge and half-integer spin, which allow for the manipulation of electron spin[2] and optically probing local electrostatic fluctuations.[3] Governed by optical selection rules different from those of excitons,[4] trions can also significantly impact the dynamics of optically forbidden dark excitons.[5] In particular, a dark-triplet exciton may be converted to a bright trion by adding an extra electron, which alters the total spin.[4] Because of their unique properties, trions have been intensively explored for a broad range of potential applications, including quantum information,[2] sensing,[3] energy harvesting,[4] lasing,[6] and light-emitting devices.[7]

However, trions have been observed only as a minority species at room temperature. In fact, although this quasi-particle was theoretically predicted by Lampert[8] as early as 1958, trions were not experimentally observed for decades until their recent identification by photoluminescence (PL) spectroscopy in low-dimensional semiconductors at cryogenic temperatures.[3,5,6,9] One of the key factors that fundamentally limits trions from being a dominant species is their low binding energy (2−45 meV).[5,9,10] In low-dimensional semiconductors, such as single-walled carbon nanotubes (SWCNTs) and atomically thin two-dimensional (2D) transition metal dichalcogenides, the binding energy of trions increases due to the stronger Coulomb interactions at reduced dimensionality, allowing trions to be detected at room temperature.[7,11] In SWCNTs, trions have been generated by high power laser excitation[11] and doping[12−15] of the host material, or by chemically charging covalently functionalized SWCNTs, as we
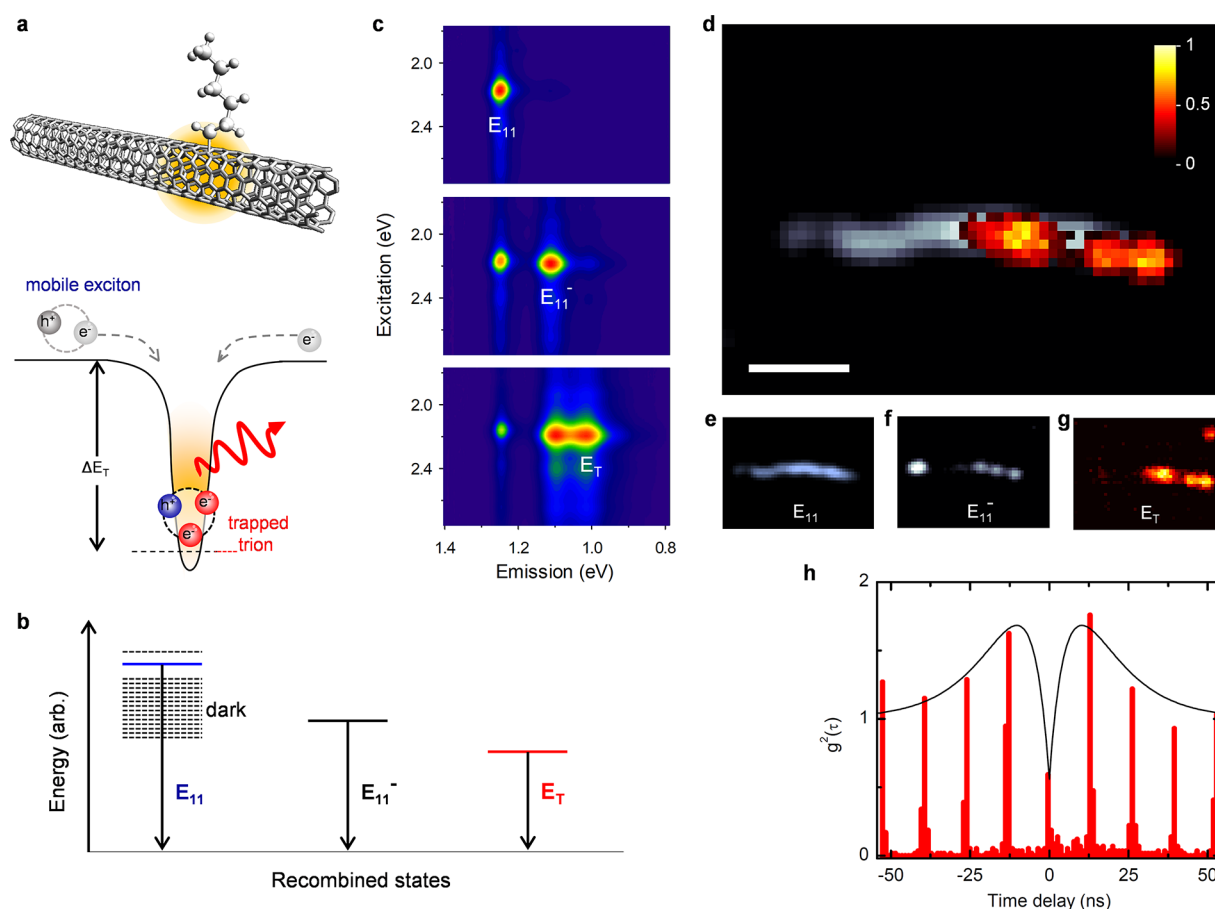
Figure 1. Spatial localization of trions at fluorescent sp^3 quantum defects. (a) Schematic of a trion trapped in a defect-induced quantum well with a depth of ΔE_T. (b) Schematic of the relative energy levels of E_{11}, E_{11}^-, and E_T in reference to the e−h recombined states. The dark states (dashed lines) are also plotted. Note that the plot is not to scale. (c) Excitation−emission PL maps showing the rise of bright trions as (6,5)-SWCNTs (top) are chemically tailored with alkyl defects and further reduced by $Na_2S_2O_4$ (middle and bottom). (d) Localized trion PL in a 4.4 μm long (6,5)-SWCNT-C_6H_{13} resolved by hyperspectral imaging. Scale bar: 2 μm. The trion PL (red) is superimposed on the E_{11} PL (light blue) of the nanotube host, with the PL intensity of E_T scaled by a factor of 4 for clarity. Hyperspectral PL images of (e) E_{11} (992 nm), (f) E_{11}^- (1108 nm), and (g) E_T (1224 nm) emission, resolved using a volumetric Bragg grating with a spectral resolution of 4 nm. (h) Photon antibunching from the E_T emission at 4.2 K.

have shown previously.[16] However, in all previous reports, including our own,[16] trion PL was still rather weak, and in the case of SWCNTs, weaker than the PL of native excitons.[12−14,16] Importantly, because of spin degeneracy and intervalley short-range Coulomb interactions in SWCNTs, the excited states of SWCNTs are dominated by dark excitonic states.[17−19] Among the 12 triplet and 4 singlet excitonic states, only the one that features singlet-spin ($S = 0$), odd-parity, and zero-angular momentum (the charge number in the K valley, N^K, equals 0) is optically allowed (bright), while the remaining 15 states are optically forbidden (dark) and 13 of which lie deeply, by ~5−100 meV, below the bright state based on quantum theory.[17−19] As a consequence, the excitation energy can be quickly lost to the dark excitonic states, unless spin−orbit coupling is negligible, and ultimately as heat. However, unlike excitons, bright trions are characterized by total spin $S = 1/2$ and $N^K = 0, 1$ (ref 4), suggesting a pathway to harness the dark-triplet excitons in SWCNTs through trion formation.

Here we report the experimental evidence of ultrabright photoluminescence from trions trapped at chemical defects that we synthetically create in semiconducting SWCNT hosts and whose well depth can be systematically tuned through the incorporation of a series of alkyl sp^3 quantum defects[20,21] into

the sp^2 carbon lattice (Figure 1a). By colocalizing a charge with the exciton at these chemically engineered defect centers, we show that it is possible to produce trions that fluoresce brightly. Through single molecule hyperspectral fluorescence imaging, we experimentally resolved strong localization of trions around defects along the nanotube host, suggesting the possibility of precise positional controlling of trion formation through chemically engineered atomic defects. Photon antibunching measurements show the emission from the trapped trions is single-photon in nature. The defect-localized trions fluoresce brightly at room temperature, even with weak excitation (<1 kW/cm^2), which is otherwise impossible in the absence of trapping-induced strong localization.[11] We experimentally determined the exciton-electron binding energy of the defect-trapped trions to be as large as 119 meV in (6,5)-SWCNTs, which is significantly larger than that of mobile trions in the same host (54 meV),[13,15] zero-dimensional (0D) quantum dots (2−25 meV),[5,9] and also 2D materials (15−45 meV),[10] and is comparable to the 327 meV binding energy of positronium anions.[1] Unlike native excitons in SWCNTs and free trions, these trapped trions are intrinsically bright (i.e., their lowest energy state is optically allowed), as revealed here by our magnetoluminescence spectroscopy and defect depend-
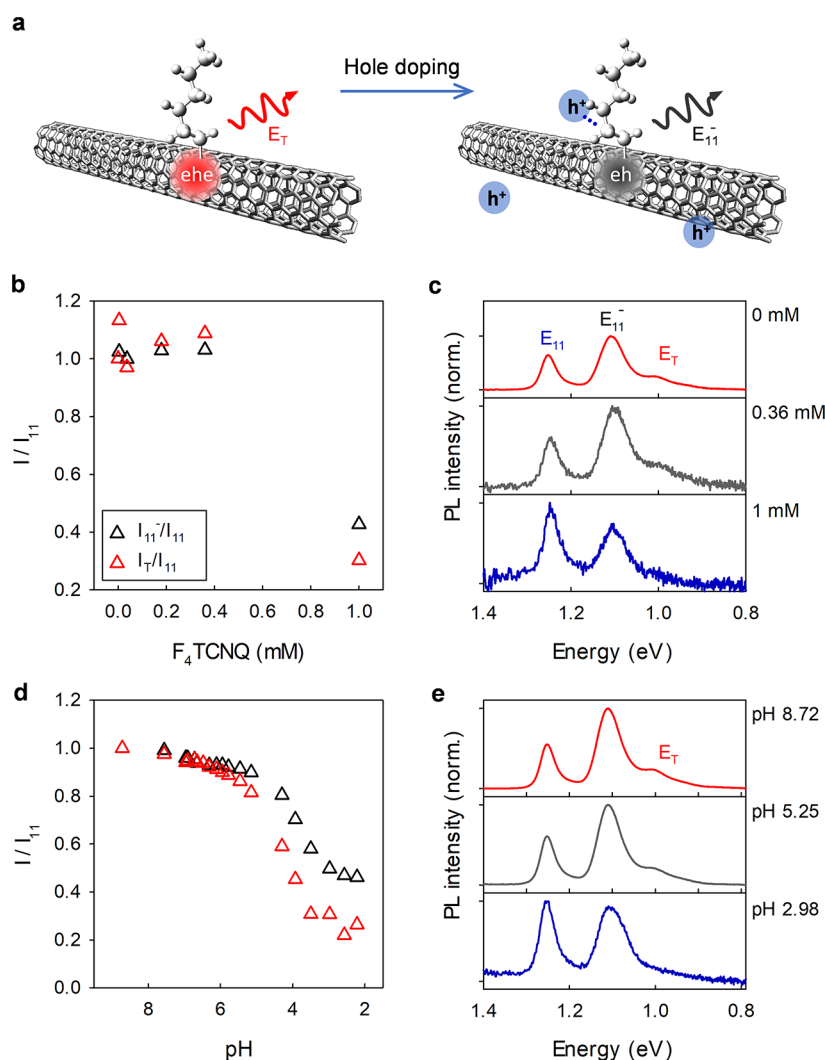
Figure 2. Hole doping of (6,5)-SWCNT-C_6H_{13} by F_4TCNQ and HCl. (a) Schematic of hole doping in SWCNT-C_6H_{13}. The hole dopants neutralize the extra negative charge of the trion, resulting in reduced E_T PL intensity. (b) The defect PL changes as a function of F_4TCNQ concentration. Note that the integrated intensity of trion PL (I_T/I_{11}) at a specific pH was normalized by the PL intensity (I_T/I_{11}) at the starting pH 8.72. (c) Normalized PL spectra of (6,5)-SWCNT-C_6H_{13} hole-doped with 0 mM (red), 0.36 mM (gray), and 1 mM (blue) of F_4TCNQ. The trion PL is completely quenched at 1 mM of F_4TCNQ. (d) The defect PL changes as a function of solution pH. (e) Normalized PL spectra of (6,5)-SWCNT-C_6H_{13} at pH 8.72 (red), 5.25 (gray), and 2.98 (blue). The trion PL completely quenched at pH 2.98.

ence studies. The trapped trions have a photoluminescence lifetime that is two orders of magnitude larger than "free" trions in the same host material, as well as an emitting probability that is surprisingly 16 times that of the native exciton, suggesting a possible pathway to brighten dark excitons through trion formation.

■ RESULTS AND DISCUSSION

Spatial Localization of Trions at sp³ Quantum Defect Sites. We chemically created sp^3 defects in the sp^2 carbon lattice of individual (6,5)-SWCNTs by covalently attaching hexyl groups to the semiconductor hosts, using a defect chemistry that we developed recently,[20] producing a 0D−1D hybrid quantum system hereafter labeled as (6,5)-SWCNT-C_6H_{13} (Figure S1). The defect creates a discrete state (E_{11}^-, emitting at 1095 nm) that lies below the native E_{11} excitonic state of the nanotube (emitting at 980 nm). $Na_2S_2O_4$, which is used as a radical initiator in the chemistry, also acts as a reducing agent that introduces electrons to the nanotube, enabling the production of negatively charged trions (E_T,

emitting at 1226 nm). The relative energy levels of E_{11}, E_{11}^-, and E_T in reference to the e−h recombined states are shown in Figure 1b. In stark contrast to free trions in unfunctionalized SWCNTs that are mobile or weakly bound at shallow potential wells,[11,15] in the presence of the introduced sp^3 defects, we found that trions are localized in a deep potential well, with a depth of ΔE_T that can be directly measured from the energy difference between E_{11} and E_T in the PL spectra (Figure 1a,b). By controlling the density of defects, the defect and trion PL intensities can also be finely tuned (Figure 1c, Figure S1).

To provide direct evidence that trions are spatially localized at the defect sites, we spectrally and spatially resolved trion PL in correlation with defects along the nanotube host (Figure 1d−g, also see Figure S2 for additional examples). Note that this observation is made at low excitation power (0.5 kW/cm^2 at an off-resonant wavelength, 730 nm) to avoid possible optical generation of trions.[11] While E_{11} PL is distributed along nearly the entire length of the imaged nanotube (7 μm), the E_{11}^- and trion PL are spatially confined within the diffraction limit of our PL microscope (430 nm for our short-wave
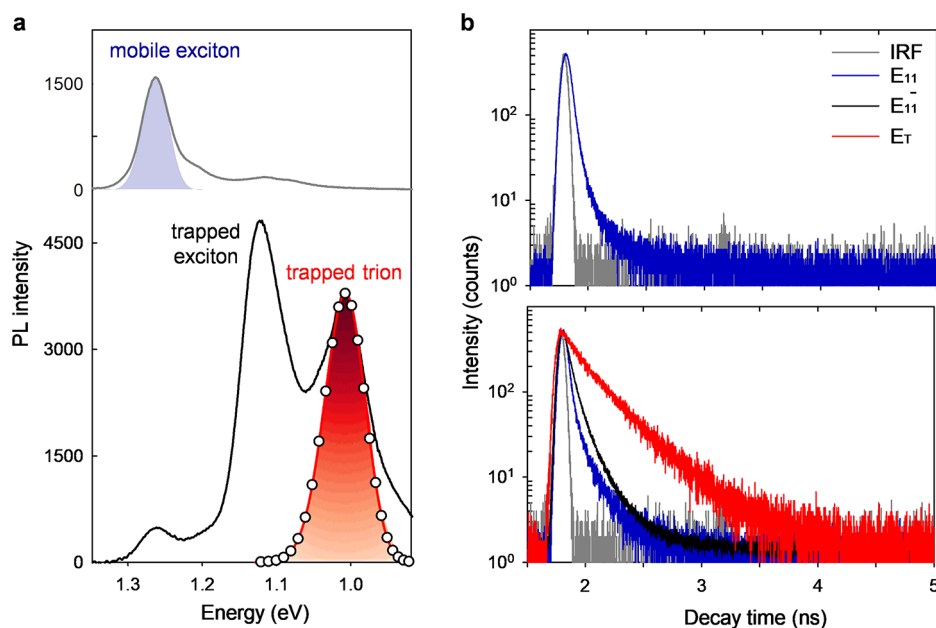
Figure 3. Ultrabright PL of defect-trapped trions. (a) PL spectra of (top) unfunctionalized (6,5)-SWCNTs and (bottom) (6,5)-SWCNT-C_6H_{13}. The excitation wavelength is 565 nm. (b) The PL decays of E_{11} from (top) (6,5)-SWCNTs and (bottom) E_T, E_{11}, and E_{11}^- of (6,5)-SWCNT-C_6H_{13} at room temperature. Note that the instrument response function (IRF) is also plotted.

infrared wavelength). The PL emission of E_T is also spatially correlated to the intensity profile of E_{11}^-, which similarly shows localization (as previously observed for excitons trapped at ether and aryl defects[22]), and at regions of the nanotube where the E_{11} PL intensity is low. This complementary nature of the intensity distribution suggests that trion PL originates from the hexyl defects and spatially correlates with E_{11}^- states.

We further show that the emission from the defect-trapped trions exhibits strong photon antibunching, which is a hallmark of single-photon emission.[23] Figure 1h is representative data obtained from a standard Hanbury−Brown−Twiss experiment on single defects in (6,5)-SWCNT-C_6H_{13} under pulsed excitation at 4.2 K. The second-order photon correlation function $g^2(\tau)$ exhibits an antibunching dip at the zero-time delay well below unity, providing strong evidence that defect-trapped trions in SWCNTs are single-photon emitters. Although antibunching is compromised by blinking, we find a single-photon purity of 0.89 by fitting the data (Figure 1h).

We note that our trion chemistry occurs at a high level of electron doping conditions induced by the reducing agent ($Na_2S_2O_4$). However, in the absence of the hexyl defects, $Na_2S_2O_4$ does not induce the charged exciton peak E_T. Controlled doping experiments further confirm that the observed E_T PL originates from negative trions in (6,5)-SWCNT-C_6H_{13} (Figure 2). Our results showed that the PL intensity of all three peaks (E_{11}, E_{11}^-, and E_T) decreased upon the addition of hydrochloric acid as a hole dopant, due to the known quenching effect of E_{11} excitons by hole doping,[24] but the E_T peak responded even more sensitively to hole doping compared to E_{11}^- (Figure 2d,e). When the proton concentration is higher than 1 mM, the trion PL becomes completely quenched. These trends are consistently observed at both low and high densities of defects (Figure S3). We also consistently observed this quenching effect for another hole doping agent, 2,3,5,6-tetrafluoro-7,7,8,8,-tetracyanoquinodimethane (Figure 2b,c), which also readily neutralizes the negatively charged trions. We note that such doping may be attained electro-

chemically, as shown in the absence of trapping defects,[12,13] or by electrically injecting electrons or holes as demonstrated in other semiconductor systems but with little positional control.[25] It is also interesting to note that with electrochemical techniques, as shown by Shiraki, Nakashima, and colleagues,[26] it may be possible to obtain additional information from the redox potential for these trapping defects. Our results here highlight that trions are generated precisely at the defect site through chemical doping of the defect.

Bright PL from Trapped Trions. In stark contrast to free trions in unfunctionalized SWCNTs,[15] our alkyl-functionalized SWCNTs exhibit surprisingly bright trion PL. In the absence of intentionally implanted defects, the PL brightness of trions is far below that of E_{11} and can only be resolved at high doping (>0.7 nm^{-1})[14] or high excitation power densities (>1 kW/cm^2).[11] Significantly, on the basis of ensemble measurements, the PL from trapped trions is significantly brighter, by approximately 7.3-fold, than the brightest trion ever reported[16] (Figure 3a). The observed trion PL intensity is even brighter, by 3.1 times, than the native E_{11} PL intensity of unfunctionalized SWCNTs, even though there are over 100 times more lattice carbon atoms than the defect sites.

PL lifetime measurements (Figure 3b and Table S2) show that the PL decay of E_{11} in (6,5)-SWCNT-C_6H_{13} is dominated by the bright state ($\tau \sim 24$ ps) and a small, long-lived component (103 ps; amplitude less than 5%). These time scales are similar to those observed in unfunctionalized control samples (25 and 147 ps), in which the long component originates from dark E_{11} excitons.[27,28] The PL decays of the defect states E_{11}^- and E_T show biexponential behavior. Interestingly, the E_T PL lifetimes (154 ± 12 ps for the short-lived component τ_s and 374 ± 8 ps for the long-lived component τ_l) are considerably longer than the E_{11} PL and "free" trions (less than 2 ps).[14] The amplitude of τ_l for E_T was 53.7 ± 1.6%, which is also significantly higher than those of E_{11} and E_{11}^- (4.8 ± 0.3% and 18.6 ± 0.4%, respectively). On the
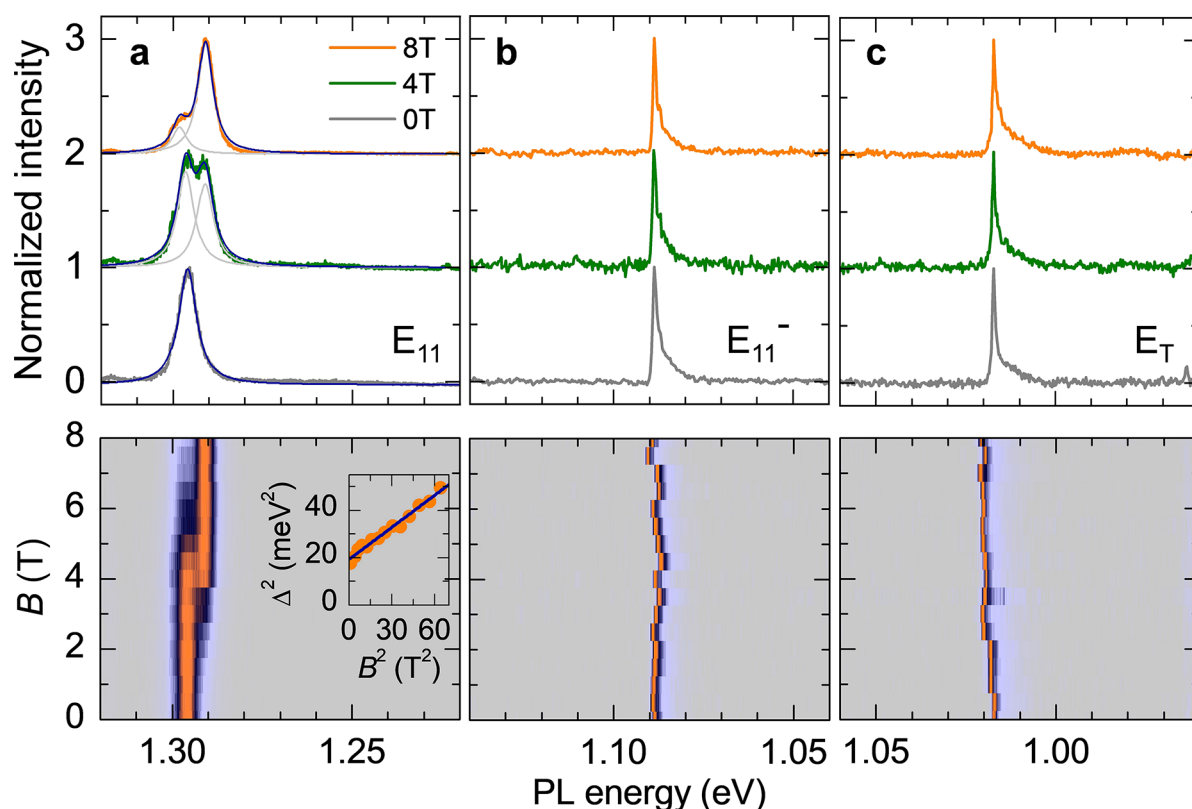
Figure 4. Spectroscopy of unfunctionalized and defect-tailored SWCNTs in a magnetic field. (a) PL spectra (upper panel) of the E_{11} emission for a single, unfunctionalized (6,5)-SWCNT without a magnetic field (gray) and in magnetic fields of 4 and 8 T (green and orange, respectively). Gray solid lines show Lorentzian fits to the bright and dark exciton peaks with their total contribution to the PL spectrum, shown as a solid blue line. The lower panel shows the color-coded PL energy dispersion of the same nanotube in magnetic fields ramped up in steps of 1 T, highlighting the transfer of the oscillator strength from the bright to dark exciton. The inset shows the evolution of the bright-dark splitting of the singlet E_{11} excitons with the Aharonov–Bohm effect induced by the magnetic field (plotted as Δ^2 vs B^2, with data fit according to $\Delta^2 = \Delta_0^2 + \Delta_{AB}^2$, shown as the solid blue line). PL spectra for the (b) E_{11}^- and (c) E_T peaks of an individual (6,5)-SWCNT-C_6H_{13}. No brightening of dark satellites was observed within the energy range of 100 meV around the E_{11}^- and E_T peaks, suggesting the absence of dark states in the energetic vicinity of the trapped excitons and trions in the sp^3 quantum defect-tailored nanotubes.

basis of fluorescent lifetime measurements, the QY of the E_{11} exciton is estimated at 1%, consistent with reports for unfunctionalized SWCNTs in aqueous dispersion.[29] To determine the emitting probability of the defect-trapped trions, we considered exciton diffusion, trapping at local defects,[27,29] and the formation of trions at the defect site, and determined that trapped trion has a probability of at least 16.3% to radiatively decay and emit a photon, which is more than 16-times as bright as the E_{11} exciton in unfunctionalized SWCNTs (see Methods in the Supporting Information).

Surprisingly, E_{11}^- and E_T are both brighter than the statistical upper-bound limit of bright E_{11} excitons in SWCNTs (which should be less than 1/16) based on spin and symmetry selection rules alone.[19] These observations suggest that brightening of dark excitons must have contributed to the observed ultrabright PL from trapped excitons and trions. By the nature of the chemistry, charge doping is localized at the defect site, thus providing a mechanism to generate trions from dark excitons that are also trapped at the defect sites. Furthermore, ΔE_T shows a strong dependence on both the nanotube chirality and diameter (Figures S4 and S5 and Table S3). The $(2n + m)$ family pattern of ΔE_T matches that of free trions in unfunctionalized SWCNTs[12] while the diameter dependence follows the inverse second-order equation, which is a signature behavior of dark excitons,[18,30] providing additional evidence that dark E_{11} excitons contribute to the

observed bright E_T emission. While our experiments do not reveal the detailed mechanism by which the dark excitons may contribute, it is possible to conclude that dark exciton brightening occurs due to the trion's extra charge, which makes this tricarrier quasi-particle follow a different selection rule from that of excitons, as discussed in the Introduction. Such a mechanism is facilitated by colocalization of dark excitons at the defect sites at which our chemistry introduces the required extra charges.

Magnetoluminescence Spectroscopy Suggests the Absence of Dark States in the Energetic Vicinity of Defect-Trapped Trions. In order to probe the presence of potential dark states in the energetic vicinity of E_{11}^- and E_T states, we performed magnetoluminescence spectroscopy on individual SWCNTs. The upper and lower panels of Figure 4a show the evolution of the E_{11} peak for an unfunctionalized (6,5)-SWCNT in response to an increasing magnetic field. The nanotube PL exhibits both characteristic features expected for an unfunctionalized SWCNT subjected to a coaxial magnetic field:[19] with increasing magnetic field, the lower-lying singlet dark state brightens progressively by acquiring oscillator strength at the expense of the bright state (as evident from the peak fits of the bright and dark PL emissions in the upper panel as well as in the color-coded PL representation in the lower panel of Figure 4a). Additionally, the bright-dark splitting of the singlet (Δ_0) evolves from its zero-field value

of 4.5 meV according to the hyperbolic relation $\Delta^2 = \Delta_0^2 + \Delta_{AB}^2$ (solid line in the inset of the lower panel of Figure 4a).[31] The field-induced energy splitting $\Delta_{AB} = \mu\varphi$ is a consequence of the Aharonov−Bohm flux $\varphi = \pi d^2 B_\parallel/4$ due to the fraction of the magnetic field $B_\parallel = B \cos\theta$ that is parallel to the SWCNT with diameter (d) and magnetic coupling constant (μ). On the basis of the fit to the data with $\theta = 45°$ for this specific nanotube, we extracted $\mu = 1.8$ meV·T^{-1} nm^{-2}, which is consistent with a (6,5) tube diameter of 0.76 nm and values found in previous experiments.[32] These results consistently suggest the presence of dark states for E_{11} excitons.

In stark contrast to the E_{11} PL of the unfunctionalized SWCNT in Figure 4a, neither the E_{11}^- nor the E_T peaks of the covalently functionalized nanotube showed sizable effects in magnetic fields of up to 8 T (upper and lower panels of Figure 4, panels b and c, respectively). Both E_{11}^- and E_T remained solitary peaks throughout the magnetic field sweep, without displaying any significant shifts or splitting within the energy boundaries given by characteristic spectral fluctuations (∼2 meV) and the resolution limit of our spectrometer (∼300 μeV), respectively.

The absence of a spin Zeeman splitting within the spectral resolution limit of our experiment can be understood by the intervalley nature of nanotube trions; i.e., the additional electron that binds to the exciton resides in the opposite valley than the electron that forms the exciton. In the absence of strong spin−orbit coupling in SWCNTs,[33] the intravalley configuration of two electrons (say both in the K valley) is energetically disfavored as compared to the intervalley configuration (one electron in K and one in K′) due to the exchange interaction. From this perspective, the extra electron is nothing but a spectator to the recombination process of an exciton without spin Zeeman splitting. In other words, since the spin projections along the magnetic field axis of the initial state (trion) and the final state (electron) are identical, the energy difference for optical transitions between these states will be effectively zero. This scenario is conceptually similar to optical transitions in monolayer 2D semiconductors, in which the magnetic-field-induced splitting is entirely due to the valley Zeeman effect, while the spin Zeeman contribution is zero.[34,35] The valley Zeeman effect in CNTs, on the other hand, is expected to be very small due to the electron−hole symmetry[36] inherited from graphene.

These observations provide the first experimental evidence that E_{11}^- and E_T are the lowest energy states for these defect-trapped quasi-particles. This further explains why the trapped excitons and trions are much brighter than their "free" counterparts, whose photophysics are dominated by non-radiative decay mechanisms due to the lower-lying dark states.[18] In contrast, the optically allowed trion can be generated from a dark-triplet exciton and an electron, presenting a new quasi-particle state that is intrinsically bright, as evidenced by the unexpected PL intensity and absence of magnetic splitting.

Large Binding Energies of Trions in Deep Trapping Wells. To better understand the origin of the defect-associated bright trions, we further determined the binding energies, E_b, of these defect-trapped quasi-particles. Because of its being localized in a deep trap, a defect-state trion is expected to have a larger binding energy due to enhanced Coulomb interactions between the exciton and electron.[37]

The binding energy of a negative trion is the minimum energy required to bind an exciton and an electron. For mobile

trions in unfunctionalized SWCNTs,[11,15] this binding energy, E_b, is determined by subtracting the energy splitting between the triplet dark E_{11} exciton, which is the lowest energy state, and the singlet bright E_{11} exciton from the energy separation, ΔE_T. By subtracting the dark-triplet bright-singlet splitting from ΔE_T (ref 17) and correcting for the dielectric constant ($\varepsilon \approx 3.5$),[38,39] we can obtain a binding energy of ∼134 meV for (6,5)-SWCNT-C$_6$H$_{13}$, compared to 54 meV for mobile trions in unfunctionalized (6,5)-SWCNTs which observe a ΔE_T of ∼178 meV[13,15] (versus 253 meV for the defect-trapped trions).

Intriguingly, as a trapped trion dissociates, either the exciton or the electron may remain trapped. Since it takes more energy for an exciton (which contains both electron and hole) than just an electron to escape the trap, the binding energy of a trapped trion would be the minimum energy required for it to dissociate into an exciton (which remains trapped at the defect) and an electron. On the energy ladder, both the trapped trion and trapped exciton are located deeply and well below that of the low-lying dark states of the E_{11} excitons (Figure 5). Furthermore, since dark states are not observed in
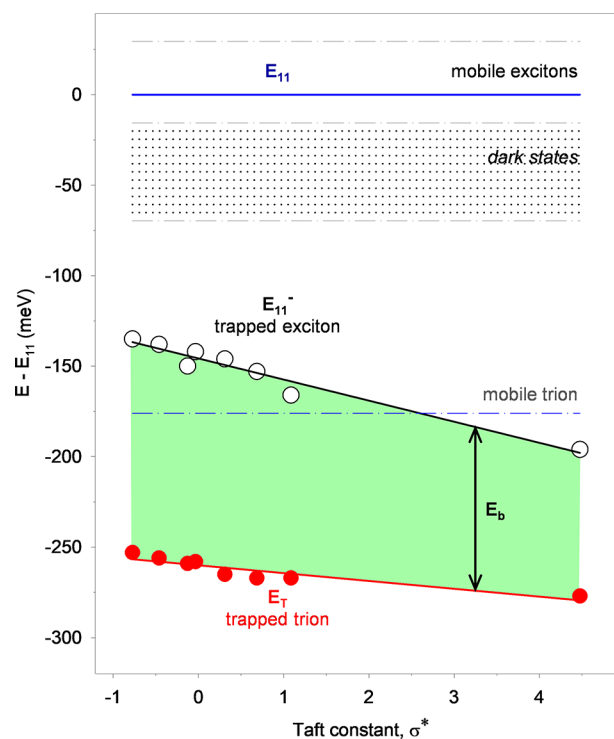

Figure 5. Binding energies of defect-trapped trions. The emission energies of E_{11}^- (black dots and line) and E_T (red dots and line) decrease linearly with the Taft constants of the functional groups that create the sp^3 quantum defects in (6,5)-SWCNTs. The bright-dark splitting of E_{11} excitons is plotted as theoretically predicted[17] energies of dark states (shaded), bound by the low-lying singlet dark state and the lowest, triplet state, which is dark. Note that these theoretical dark state energies are not corrected for the difference in dielectric environment of our experimental systems. The energy level of the mobile trion[15] is also plotted for comparison.

the energy vicinity of the trapped trion or trapped exciton, the lowest energy state is optically allowed for both excitons and trions when they are trapped at a sp^3 defect. Therefore, the binding energy of the trapped trion is simply the energy difference between the trapped trion and trapped exciton, which can be experimentally determined directly from E_T and

Table 1. Binding Energy of Trions in (6,5)-SWCNT-R Depends on the Chemical Nature of the sp^3 Quantum Defect[a]

R	σ_{calc}	E_{11} (nm)	E_{11}^- (nm)	E_T (nm)	ΔE_T (meV)	E_b (meV)
-$(CF_2)_2(CF_2)_3CF_3$	4.48	986	1168	1265	277	81
-$(CH_2)_2(CF_2)_3CF_3$	1.09	984	1133	1248	267	101
-$(CF_2)_2CF_2CF_3$	0.69	978	1112	1239	267	114
-$(CH_2)_2CF_3$	0.31	980	1108	1240	265	119
-$(CH_2)_2CH_2CF_3$	−0.03	980	1104	1231	258	116
-$(CF_2)_4CF_2CF_3$	−0.13	980	1112	1232	259	109
-$(CH_2)_2(CH_2)_3CF_3$	−0.46	980	1100	1229	256	118
-$(CH_2)_2(CH_2)_3CH_3$	−0.77	981	1098	1227	253	119

[a]Note that σ_{calc} is the Taft constant for each alkyl functional group calculated based on an empirical formula.[43]

E_{11}^- to be 119 meV. This binding energy is slightly lower than that derived from the conventional picture (134 meV) which makes use of theoretically predicted dark-bright splitting energy and dielectric constants. Even with this conservative lower-bound value (119 meV), the binding energy of a trapped trion is significantly larger than that of mobile trions in unfunctionalized (6,5)-SWCNTs (54 meV),[13,15] 0D quantum dots (2−25 meV),[5,9] and 2D materials (15−45 meV).[10]

This large binding energy explains the unexpected brightness observed for trapped trions. By systematically varying the chemical nature of the defects, ranging from nonfluorinated (−C_6H_{13}), partially fluorinated, and perfluorinated (−C_6F_{13}), we found it is possible to tune the well depth and the binding energy of the trapped trion (Figure 5, Table 1). We also observed that the E_T PL becomes weaker with increasing depth of the potential well, as indicated by E_{11}^- (Figure S6). This observation was initially unexpected, but can be understood as a result of the electronic inductive effects of fluorine on the alkyl defects and can be quantitatively correlated to the Taft constant, σ^* (ref 20). On one hand, the fluorine deepens the exciton trapping potential, resulting in the larger energy shift for E_{11}^-. On the other hand, with its electron withdrawing capability the fluorine may pull electron density away from the trapped trion, and as a consequence E_b of the trapped trion decreases by 38 meV for (6,5)-SWCNT-C_6F_{13} compared to the -C_6H_{13} defects. Extrapolating the E_{11}^- and E_T curves in Figure 5, we suspect that the trion may lose brightness further when σ^* becomes significantly more positive, since the binding energy may decrease to a level inadequate to bind the electron−hole−electron as a quasi-particle. This inductive effect suggests the possibility of electrically gating the generation of excitons and trions at chemically incorporated defect sites, which will be verified in future experiments.

CONCLUSION

We observed ultrabright PL from trions trapped at sp^3 defects that were synthetically created in semiconducting SWCNT hosts by covalent bonding of alkyl groups to the sp^2 carbon lattice. The trapped trion is 16 times as bright as the native nanotube excitons, with a photoluminescence lifetime that is more than 100 times greater than "free" trions in the same host material. This unexpected brightness arises from strong localization of the trion in the deep potential well of the defect, as supported by single nanotube photoluminescence imaging, giving rise to an extraordinarily large exciton-electron binding energy (119 meV in (6,5)-SWCNT-C_6H_{13}). Magneto-luminescence spectroscopy suggests that the lowest energy states for these defect-trapped tricarrier quasi-particles are optically allowed. With the efficient generation of ultrabright trions, it is now possible to manipulate charged excitons with

nonzero spin, which provides an ideal platform for studying fundamental photophysics, including dark exciton states in low-dimensional carbon materials and many-body physics. The strong localization makes trions readily accessible through chemically introduced defects, enabling positional control over the charging chemistry that allows trion formation to occur precisely at the trapping defect. To our knowledge, this type of control has not been possible in the solid-state nanostructures previously studied.[3,5,12−15,25] Many promising applications derived from these materials can also be expected, including infrared bioimaging,[40] carrier-doped field effect transistors,[12,13] and quantum information science.[2,41]

METHODS

High Purity SWCNT Hosts. CoMoCAT SG65i (Southwest Nanotechnologies, lot no. SG65i-L39) were stabilized in water as individual nanotubes and sorted to single chirality purity. The sorted SWCNTs were stabilized in D_2O (Cambridge Isotope Laboratories, Inc., 99.8%) with 1 wt %/v sodium dodecyl sulfate (Sigma-Aldrich, >98.5%) for subsequent functionalization.

Chemical Creation of sp^3 Defects in SWCNT Hosts. To incorporate sp^3 defects, 7.6 mM NaHCO$_3$ (EMD chemicals, HPLC grade), 0.16% v/v CH$_3$CN (Acros organics, HPLC grade, 99.9%), and various alkyl halides (see Table S1), and 3.6 mM of Na$_2$S$_2$O$_4$ (Sigma-Aldrich, 85%) were added sequentially to each SWCNT solution and reacted for 2 h. To increase the density of defects, the concentration of the alkyl halide was increased proportionally to the concentration of the SWCNTs.

Spectroscopic Characterization of Trion PL. The reactions were monitored in situ using a NanoLog spectrofluorometer (HORIBA Jobin Yvon). The samples were excited with a 450 W xenon source dispersed by a double-grating monochromator. The slit width of the excitation and emission beams was 10 nm. Excitation−emission maps and single excitation PL spectra were collected using a liquid-N$_2$ cooled linear InGaAs array detector. Absorption spectra were measured using a Lambda 1050 UV-vis-NIR spectrophotometer (PerkinElmer) equipped with both a photomultiplier tube and an extended InGaAs detector. For single tube PL imaging, a small aliquot of (6,5)-SWCNT-C_6H_{13} solution in 1% wt/v sodium deoxycholate (Sigma-Aldrich, > 99%) was deposited on poly D-lysine coated glass slides (part no. P35GC-0-10-C, MatTek Corporation). The imaging was performed using a custom-built microscope that integrates a volume Bragg grating system (Photon etc) and an oil immersion objective (UAPON 150XOTIRF, NA = 1.45, Olympus).[42] The nanotubes were excited by a 730 nm diode laser at a power density of 0.5 kW/cm^2, and the PL emission was collected using a liquid-N$_2$

cooled 2D InGaAs detector array (Cougar 640, Xenics) with an integration time of 16 s.

Hole Doping Experiments. The (6,5)-SWCNT-C_6H_{13} solutions were ultrafiltrated using a 100 kDa ultrafiltration centrifugal tube (Amicon, EMD Millipore) to remove the reaction byproducts and unreacted reagents. The sp^3 quantum defect-tailored SWCNTs were then hole-doped by hydrochloric acid. The solution pH was adjusted from 2.98 to 8.72 by adding small aliquots of 20 mM HCl (Sigma-Aldrich) or NaHCO$_3$ solutions. The pH was determined using a pH meter (Accumet AB15+ Basic and BioBasic pH meters, Fisher Scientific). Hole doping by 2,3,5,6-tetrafluoro-7,7,8,8-tetracyanoquinodimethane (F$_4$TCNQ) was performed by sequentially increasing the concentration of F$_4$TCNQ (Sigma-Aldrich, 97%, lot no. MKBR1477 V) from 0 to 1 mM in the SWCNT solution.

PL Lifetime Measurements. The PL lifetimes were measured at room temperature using 568 nm excitation (4 ps pulsewidth, 40 MHz repetition rate) and a single quantum nanowire detector. Spectral filtering to resolve each PL peak was achieved with appropriate band-pass (BP)/long-pass (LP) filters in front of the detector, including BP 1000/50 for E_{11}, BP 1100/10 for E_{11}^-, and LP1200 for E_T. The collected decay curves were reconvolution fitted with the corresponding instrument response function for each detector in FluoFit (Picoquant).

Magnetoluminescence Measurements. The unfunctionalized (6,5)-SWCNT control and (6,5)-SWCNT-C_6H_{13} in 1% wt/v DOC were drop-cast onto SiO$_2$ substrates and subjected to magnetic fields of up to 8 T in a home-built confocal microscope immersed in a helium bath cryostat with a base temperature of 4.2 K. Individual nanotubes were selected for collinear orientation with the magnetic field axis using the well-known antenna effect.

Safety Statement. No unexpected or unusually high safety hazards were encountered.

ASSOCIATED CONTENT

Ⓢ Supporting Information

The Supporting Information is available free of charge on the ACS Publications website at DOI: 10.1021/acscentsci.9b00707.

Detailed methods, Raman scattering, absorption spectra, and additional PL data (Figures S1−S6 and Tables S1−S3) (PDF)

AUTHOR INFORMATION

Corresponding Author

*E-mail: yhw@umd.edu.

ORCID Ⓞ

Hyejin Kwon: 0000-0003-0548-6970
Mijin Kim: 0000-0002-7781-9466
Nicolai F. Hartmann: 0000-0002-4174-532X
Han Htoon: 0000-0003-3696-2896
Stephen K. Doorn: 0000-0002-9535-2062
Alexander Högele: 0000-0002-0178-9117
YuHuang Wang: 0000-0002-5664-1849

Author Contributions

#H.K. and M.K. contributed equally to this work.

Author Contributions

Y.H.W., H.K., and M.K. conceived and designed the experiments. H.K. and M.K. performed the synthesis and spectroscopy characterization. N.F., H.H., and S.K.D. performed fluorescent lifetime measurements. M.N., V.P., M.S.H., and A.H. performed magnetoluminescence measurements. B.M. performed gel purification. All the authors contributed to the discussions and preparation of the manuscript.

Notes

The authors declare no competing financial interest.

REFERENCES

(1) Nagashima, Y. Experiments on positronium negative ions. *Phys. Rep.* **2014**, *545* (3), 95−123.

(2) De Greve, K.; Yu, L.; McMahon, P. L.; Pelc, J. S.; Natarajan, C. M.; Kim, N. Y.; Abe, E.; Maier, S.; Schneider, C.; Kamp, M.; Hofling, S.; Hadfield, R. H.; Forchel, A.; Fejer, M. M.; Yamamoto, Y. Quantum-dot spin-photon entanglement via frequency downconversion to telecom wavelength. *Nature* **2012**, *491* (7424), 421−425.

(3) Brinkmann, D.; Kudrna, J.; Gilliot, P.; Hönerlage, B.; Arnoult, A.; Cibert, J.; Tatarenko, S. Trion and exciton dephasing measurements in modulation-doped quantum wells: A probe for trion and carrier localization. *Phys. Rev. B: Condens. Matter Mater. Phys.* **1999**, *60* (7), 4474−4477.

(4) Watanabe, K.; Asano, K. Trions in semiconducting single-walled carbon nanotubes. *Phys. Rev. B: Condens. Matter Mater. Phys.* **2012**, *85* (3), 035416.

(5) Patton, B.; Langbein, W.; Woggon, U. Trion, biexciton, and exciton dynamics in single self-assembled CdSe quantum dots. *Phys. Rev. B: Condens. Matter Mater. Phys.* **2003**, *68* (12), 125316.

(6) Puls, J.; Mikhailov, G. V.; Henneberger, F.; Yakovlev, D. R.; Waag, A.; Faschinger, W. Laser action of trions in a semiconductor quantum well. *Phys. Rev. Lett.* **2002**, *89* (28), 287402.

(7) Zhang, Y. J.; Oka, T.; Suzuki, R.; Ye, J. T.; Iwasa, Y. Electrically switchable chiral light-emitting transistor. *Science* **2014**, *344* (6185), 725−728.

(8) Lampert, M. A. Mobile and immobile effective-mass-particle complexes in nonmetallic solids. *Phys. Rev. Lett.* **1958**, *1* (12), 450−453.

(9) Bracker, A. S.; Stinaff, E. A.; Gammon, D.; Ware, M. E.; Tischler, J. G.; Park, D.; Gershoni, D.; Filinov, A. V.; Bonitz, M.; Peeters, F.; Riva, C. Binding energies of positive and negative trions: From quantum wells to quantum dots. *Phys. Rev. B: Condens. Matter Mater. Phys.* **2005**, *72* (3), 035332.

(10) Zhang, D. K.; Kidd, D. W.; Varga, K. Excited biexcitons in transition metal dichalcogenides. *Nano Lett.* **2015**, *15* (10), 7002−7005.

(11) Santos, S. M.; Yuma, B.; Berciaud, S.; Shaver, J.; Gallart, M.; Gilliot, P.; Cognet, L.; Lounis, B. All-optical trion generation in single-walled carbon nanotubes. *Phys. Rev. Lett.* **2011**, *107* (18), 187401.

(12) Park, J. S.; Hirana, Y.; Mouri, S.; Miyauchi, Y.; Nakashima, N.; Matsuda, K. Observation of negative and positive trions in the electrochemically carrier-doped single-walled carbon nanotubes. *J. Am. Chem. Soc.* **2012**, *134* (35), 14461−14466.

(13) Jakubka, F.; Grimm, S. B.; Zakharko, Y.; Gannott, F.; Zaumseil, J. Trion electroluminescence from semiconducting carbon nanotubes. *ACS Nano* **2014**, *8* (8), 8477−8486.

(14) Koyama, T.; Shimizu, S.; Miyata, Y.; Shinohara, H.; Nakamura, A. Ultrafast formation and decay dynamics of trions in p-doped single-walled carbon nanotubes. *Phys. Rev. B: Condens. Matter Mater. Phys.* **2013**, *87* (16), 165430.

(15) Matsunaga, R.; Matsuda, K.; Kanemitsu, Y. Observation of charged excitons in hole-doped carbon nanotubes using photoluminescence and absorption spectroscopy. *Phys. Rev. Lett.* **2011**, *106* (3), 037404.

(16) Brozena, A. H.; Leeds, J. D.; Zhang, Y.; Fourkas, J. T.; Wang, Y. Controlled defects in semiconducting carbon nanotubes promote efficient generation and luminescence of trions. *ACS Nano* **2014**, *8* (5), 4239−4247.

(17) Spataru, C. D.; Ismail-Beigi, S.; Capaz, R. B.; Louie, S. G. Theory and ab Initio calculation of radiative lifetime of excitons in semiconducting carbon nanotubes. *Phys. Rev. Lett.* **2005**, *95* (24), 247402.

(18) Capaz, R. B.; Spataru, C. D.; Ismail-Beigi, S.; Louie, S. G. Diameter and chirality dependence of exciton properties in carbon nanotubes. *Phys. Rev. B: Condens. Matter Mater. Phys.* **2006**, *74* (12), 121401.

(19) Ando, T. Effects of valley mixing and exchange on excitons in carbon nanotubes with Aharonov−Bohm flux. *J. Phys. Soc. Jpn.* **2006**, *75* (2), 024707.

(20) Kwon, H.; Furmanchuk, A. o.; Kim, M.; Meany, B.; Guo, Y.; Schatz, G. C.; Wang, Y. Molecularly tunable fluorescent quantum defects. *J. Am. Chem. Soc.* **2016**, *138* (21), 6878−6885.

(21) Brozena, A. H.; Kim, M.; Powell, L. R.; Wang, Y. Controlling the optical properties of carbon nanotubes with organic colour-centre quantum defects. *Nat. Rev. Chem.* **2019**, *3* (6), 375−392.

(22) Hartmann, N. F.; Yalcin, S. E.; Adamska, L.; Haroz, E. H.; Ma, X.; Tretiak, S.; Htoon, H.; Doorn, S. K. Photoluminescence imaging of solitary dopant sites in covalently doped single-wall carbon nanotubes. *Nanoscale* **2015**, *7* (48), 20521−20530.

(23) Högele, A.; Galland, C.; Winger, M.; Imamoğlu, A. Photon antibunching in the photoluminescence spectra of a single carbon nanotube. *Phys. Rev. Lett.* **2008**, *100* (21), 217401.

(24) Crochet, J. J.; Duque, J. G.; Werner, J. H.; Doorn, S. K. Photoluminescence imaging of electronic-impurity-induced exciton quenching in single-walled carbon nanotubes. *Nat. Nanotechnol.* **2012**, *7* (2), 126−132.

(25) Ross, J. S.; Wu, S.; Yu, H.; Ghimire, N. J.; Jones, A. M.; Aivazian, G.; Yan, J.; Mandrus, D. G.; Xiao, D.; Yao, W.; Xu, X. Electrical control of neutral and charged excitons in a monolayer semiconductor. *Nat. Commun.* **2013**, *4*, 1474.

(26) Shiraishi, T.; Shiraki, T.; Nakashima, N. Substituent effects on the redox states of locally functionalized single-walled carbon nanotubes revealed by in situ photoluminescence spectroelectrochemistry. *Nanoscale* **2017**, *9* (43), 16900−16907.

(27) Hartmann, N. F.; Velizhanin, K. A.; Haroz, E. H.; Kim, M.; Ma, X.; Wang, Y.; Htoon, H.; Doorn, S. K. Photoluminescence dynamics of aryl sp³ defect states in single-walled carbon nanotubes. *ACS Nano* **2016**, *10* (9), 8355−8365.

(28) Berciaud, S.; Cognet, L.; Lounis, B. Luminescence decay and the absorption cross section of individual single-walled carbon nanotubes. *Phys. Rev. Lett.* **2008**, *101* (7), 077402.

(29) Miyauchi, Y.; Iwamura, M.; Mouri, S.; Kawazoe, T.; Ohtsu, M.; Matsuda, K. Brightening of excitons in carbon nanotubes on dimensionality modification. *Nat. Photonics* **2013**, *7* (9), 715−719.

(30) Piao, Y.; Meany, B.; Powell, L. R.; Valley, N.; Kwon, H.; Schatz, G. C.; Wang, Y. Brightening of carbon nanotube photoluminescence through the incorporation of sp³ defects. *Nat. Chem.* **2013**, *5* (10), 840−845.

(31) Shaver, J.; Kono, J.; Portugall, O.; Krstić, V.; Rikken, G. L. J. A.; Miyauchi, Y.; Maruyama, S.; Perebeinos, V. Magnetic brightening of carbon nanotube photoluminescence through symmetry breaking. *Nano Lett.* **2007**, *7* (7), 1851−1855.

(32) Srivastava, A.; Htoon, H.; Klimov, V. I.; Kono, J. Direct observation of dark excitons in individual carbon nanotubes: Inhomogeneity in the exchange splitting. *Phys. Rev. Lett.* **2008**, *101* (8), 087402.

(33) Kuemmeth, F.; Ilani, S.; Ralph, D. C.; McEuen, P. L. Coupling of spin and orbital motion of electrons in carbon nanotubes. *Nature* **2008**, *452*, 448−452.

(34) Li, Y.; Ludwig, J.; Low, T.; Chernikov, A.; Cui, X.; Arefe, G.; Kim, Y. D.; van der Zande, A. M.; Rigosi, A.; Hill, H. M.; Kim, S. H.; Hone, J.; Li, Z.; Smirnov, D.; Heinz, T. F. Valley splitting and polarization by the Zeeman effect in monolayer MoSe₂. *Phys. Rev. Lett.* **2014**, *113* (26), 266804.

(35) Srivastava, A.; Sidler, M.; Allain, A. V.; Lembke, D. S.; Kis, A.; Imamoğlu, A. Valley Zeeman effect in elementary optical excitations of monolayer WSe₂. *Nat. Phys.* **2015**, *11*, 141−147.

(36) Jarillo-Herrero, P.; Sapmaz, S.; Dekker, C.; Kouwenhoven, L. P.; van der Zant, H. S. J. Electron-hole symmetry in a semiconducting carbon nanotube quantum dot. *Nature* **2004**, *429*, 389−392.

(37) Bondarev, I. V. Relative stability of excitonic complexes in quasi-one-dimensional semiconductors. *Phys. Rev. B: Condens. Matter Mater. Phys.* **2014**, *90* (24), 245430.

(38) Rønnow, T. F.; Pedersen, T. G.; Cornean, H. D. Correlation and dimensional effects of trions in carbon nanotubes. *Phys. Rev. B: Condens. Matter Mater. Phys.* **2010**, *81* (20), 205446.

(39) Capaz, R. B.; Spataru, C. D.; Ismail-Beigi, S.; Louie, S. G. Excitons in carbon nanotubes: Diameter and chirality trends. *Phys. Status Solidi B* **2007**, *244* (11), 4016−4020.

(40) Hong, G.; Diao, S.; Antaris, A. L.; Dai, H. Carbon nanomaterials for biological imaging and nanomedicinal therapy. *Chem. Rev.* **2015**, *115* (19), 10816−10906.

(41) He, X.; Hartmann, N. F.; Ma, X.; Kim, Y.; Ihly, R.; Blackburn, J. L.; Gao, W.; Kono, J.; Yomogida, Y.; Hirano, A.; Tanaka, T.; Kataura, H.; Htoon, H.; Doorn, S. K. Tunable room-temperature single-photon emission at telecom wavelengths from sp³ defects in carbon nanotubes. *Nat. Photonics* **2017**, *11*, 577−582.

(42) Wu, X.; Kim, M.; Qu, H.; Wang, Y. Single-defect spectroscopy in the shortwave infrared. *Nat. Commun.* **2019**, *10* (1), 2672.

(43) Cherkasov, A. R; Galkin, V. I; Cherkasov, R. A The problem of the quantitative evaluation of the inductive effect: correlation analysis. *Russ. Chem. Rev.* **1996**, *65* (8), 641.